Ventral striatal atrophy in Alzheimer's disease : exploring a potential new imaging marker for early dementia

Jong, L.W. de

CHAPTER 3

Shape abnormalities of the striatum in AD

Laura W de Jong

Luca Ferrarini

Jeroen van der Grond

Julien R Milles

Johan HC Reiber

Rudi GJ Westendorp

Edward LEM Bollen

Huub AM Middelkoop

Mark A van Buchem

Adapted from J Alzheimers Dis. 2011;23(1):49-59. doi: 10.3233/JAD-2010-101026.

ABSTRACT

Post mortem studies show pathological changes in the striatum in Alzheimer's disease (AD). Here, we examine the surface of the striatum in AD and assess whether changes of the surface are associated with impaired cognitive functioning. The shape of the striatum (nucleus accumbens, caudate nucleus, and putamen) was compared between 35 AD patients and 35 individuals without cognitive impairment. The striatum was automatically segmented from 3D T1 magnetic resonance images and automatic shape modeling tools (Growing Adaptive Meshes) were applied for morphometric analysis. Repeated permutation tests were used to identify locations of consistent shape deformities of the striatal surface in AD. Linear regression models, corrected for age, gender, educational level, head size, and total brain parenchymal volume were used to assess the relation between cognitive performance and local surface deformities. In AD patients, differences of shape were observed on the medial head of the caudate nucleus and on the ventral lateral putamen, but not on the accumbens. The head of the caudate nucleus and ventral lateral putamen are characterized by extensive connections with the orbitofrontal and medial temporal cortices. Severity of cognitive impairment was associated with the degree of deformity of the surfaces of the accumbens, rostral medial caudate nucleus, and ventral lateral putamen. These findings provide further evidence for the hypothesis that in AD primarily associative and limbic cerebral networks are affected.

INTRODUCTION

Histological studies have demonstrated pathological changes in the striatum of Alzheimer's disease (AD) patients. These changes comprise the presence of diffuse plaques throughout the striatum (Gearing, Levey, and Mirra 1997) and the presence of neurofibrillary tangles in mainly large striatal nerve cells (Oyanagi et al. 1991; Oyanagi et al. 1987). In *in vivo* studies, using magnetic resonance imaging (MRI), atrophy has been observed in the caudate nucleus (Karas et al. 2003) and putamen (de Jong et al. 2008) of AD patients. Furthermore, evidence for the occurrence of striatal degeneration early in the development of AD is accumulating. In a structural MRI study, atrophy of the basal forebrain, including the ventral striatum, has been found to precede the development of dementia (Hall et al. 2008). In a Pittsburgh compound B positron emission tomography study of a familial form of AD, amyloid depositions have been observed well before the onset of cognitive symptoms (Klunk et al. 2007) and . It is not known, however, whether striatal atrophy is a diffuse process or limited to parts of the striatum and whether it relates to impaired performance on certain cognitive tasks.

The human striatum comprises the nucleus accumbens, caudate nucleus, and putamen and is regarded as the major input nucleus of the basal ganglia, receiving afferents from the entire cortex, thalamus, and substantia nigra. Efferents from the striatum run to the internal and external parts of the globus pallidus, subthalamic nucleus, and substantia nigra pars reticulata, and from these structures output pathways arise to the thalamus, superior colliculus and pedunculopontine tegmental nucleus (Gerfen 1992). Via the thalamus feedback is given to the striatum and cortex, predominantly the frontal cortex (Herrero, Barcia, and Navarro 2002). The striatum contains limbic, associative, and sensorimotor subregions, a division derived from the connections with functionally different cortical areas. This functional subdivision does not follow the anatomical boundaries such as those between caudate and putamen, but exerts a ventromedial to dorsolateral gradient (Voorn et al. 2004).

Knowledge on the functions of the basal ganglia is also based on observations in pathological conditions and experimental animal studies. Basal ganglia diseases lead to profound motor and cognitive disorders; for instance dyskinesia in Huntington's disease, diminished motor function and initiation of motor tasks in Parkinson's disease, tics in Tourette's syndrome, and recurrent obsessions and compulsions in obsessive compulsive disorders (Utter and Basso 2008). Lesions in the striatum give rise to diverse motor and cognitive disturbances, most commonly dystonia and abulia (Bhatia and Marsden 1994). Based on these clinical observations, the striatum is believed to play an important role in choosing and switching between competing behaviors (Parkinson et al. 2000), reinforcement learning processes (Poldrack and Packard 2003), procedural memory and

habit formation (Graybiel 2008), and working memory (Landau et al. 2009). Due to the variety of networks the striatum takes part in and due to the variety of functions of different parts of the striatum, the location of pathological changes within the striatum may determine the symptoms that arise. A region-specific approach is therefore critical when studying the striatum. Volumetric analyses are limited to a crude division of the striatum along anatomical landmarks, which disregards the functional heterogeneity of the structure. Furthermore, contrast differences on MRI within the striatum are insufficient to identify different functional parts. Shape analysis, however, captures details on locations of atrophy and allows a regional assessment of areas related to cognitive symptoms along the surface of the structure.

Here, we further investigated the involvement of the striatum in AD and possible association with cognitive performance. The striatal shapes of 35 AD patients to those of 35 memory complainers (MCs) with normal cognitive test scores were compared. First, the locations of consistent significant shape changes in AD were assessed. Secondly, the degree of local surface deformities was related to performance on the Cambridge Cognitive Examination-Revised (CAMCOG-R). We postulate that especially the ventral striatal areas, anatomically connected to functional networks mostly affected in AD, i.e., the limbic and associative cortices, would show atrophy in AD. In addition, we postulated that shape abnormalities in these same areas related to impaired cognitive performance.

METHODS

Subjects and study design

Study and control subjects were recruited from the population who visited the outpatient's memory clinic of our institution between January 1, 2006 and May 1, 2008. Each subject was examined according to a standardized protocol, including a whole brain MRI examination, neuropsychological screening (including the CAMCOG-R (Roth et al. 1988), a screening test for cognitive performance, and Geriatric Depression Scale (GDS) (Yesavage and Sheikh 1986), and a general medical and neurological examination by a geriatrician and neurologist respectively. Per subject, all tests took place within a 2-week span. In a multidisciplinary meeting, patients with abnormal test results were diagnosed with possible or probable AD, other types of dementia, mild cognitive impairment (MCI), or a neurological or psychiatric disorder. The National Institute of Neurological and Communicative Disorders and Stroke and Alzheimer's Disease and Related Disorders Association (NINCDS-ADRDA) criteria were applied for diagnosing probable AD (pAD) (McKhann et al. 1984). Subjects with normal results on all cognitive tests were classified as memory complainers (MCs). Identified reasons for subjective memory

impairment experienced by the memory complainers included mild or severe depressions, and emotional psychosocial events such as the loss of a family member or problems at work. For over half of the memory complainers no explanation for the experienced memory decline was identified. For the current study, we excluded the following subjects from the entire population ($n = 399$): left-handed subjects ($n = 35$), people with cognitive deficits who did not meet the criteria for probable AD, including the category of MCI ($n = 141$); other forms of dementia ($n = 11$) e.g., frontotemporal dementia, Lewy body disease, vascular dementia, Parkinson's dementia; other neurological/psychiatric disorders ($n = 35$), e.g., normal pressure hydrocephalus, intracranial tumors, stroke etc.; severe mood disorders with GDS > 10; alcohol abuse (n=8); insufficient scan quality ($n = 4$). In order to minimalize confounding effects in the shape analysis we selected from the remaining population ($n = 165$) two complete data sets of 35 probable AD patients and 35 MCs that matched in age, gender and years of education. The institutional review board of the Leiden University Medical Center approved this cross-sectional case-control study.

Magnetic Resonance data acquisition

MRI was performed using a 3.0 Tesla whole body MRI scanner (Philips Medical Systems, Best, The Netherlands) with a Sense HEAD 8 channel coil. 3D T1-weighted MR images were coronally acquired with voxel dimensions: 0.875 mm (left-right) $\times$ 0.875 mm (feet-head) $\times$ 1.4 mm (anterior-posterior). Phase encoding directions were anterior-posterior and left-right, and frequency encoding direction was feet-head. Remaining settings were: TR = 9.8 ms; TE = 4.6 ms; flip angle = 8°; section thickness = 1.2 mm; number of sections = 120; no section gap; whole brain coverage; FOV = 224 mm; matrix = 192, reconstruction matrix = 256×256. CLEAR inhomogeneity correction was applied. Routine T2-weighted and fluid attenuated inversion recovery (FLAIR) weighted scans were performed to identify out large infarcts and mass lesions.

Automated segmentation of the striatum

Automated segmentation and volume estimation of the nucleus accumbens, caudate nucleus, putamen, and globus pallidus was performed using FIRST (FMRIB's Integrated Registration and Segmentation Tool) (Patenaude et al. 2007), part of FMRIB's Software Library (FSL) (SM Smith, Jenkinson, et al. 2004). We used the *run_first_all* script with default options, followed by a boundary correction with z=3. The segmentations of nucleus accumbens, caudate nucleus, and putamen were combined to form the striatum. All segmentations of our study sample were visually inspected for errors,

but none were found. SIENAX (Structural Image Evaluation, using Normalization, of Atrophy, X-sectional), also part of FSL, was used to estimate global brain tissue volumes (SM Smith, De Stefano, et al. 2001; SM Smith, Zhang, et al. 2002) and a scaling factor, used for normalization for head size.

Assessment of the relation of striatal volumes and cognitive performance

R 2.10.1 was used for data analysis (R Core Team 2009). Differences in mean age, gender, education in years, head size normalization factor, brain parenchymal volume (BPV), CAMCOG-R scores, and striatal volumes were tested by a two sample unpaired t-test. Relations of striatal volumes, normalized for head size, with cognition were also estimated. First corrections for age, gender, educational level, and BPV were made by means of linear regression analysis: expected values of CAMCOG-R score were calculated from regression of CAMCOG-R score on age, gender, education in years. Subsequently, residuals were correlated to normalized volumes of total striatum, caudate, putamen and nucleus accumbens. A p-value $\leqslant 0.05$ was considered statistically significant.

Morphometric analysis of the striatum

Comparison of striatal shapes of AD and MC

Shape modeling The striatal segmentations by FIRST, registered to MNI (Montreal Neurological Institute) 152 standard space by means of affine transformation with 12 degrees of freedom, were used for quantitative analysis of local shape changes. Growing and Adaptive MEshes (GAMEs) method was adopted, which has been described previously and discussed here in essence (Ferrarini, Olofsen, et al. 2007). Left and right striatal hemisphere were separately analyzed, each formed by combining the caudate nucleus, putamen, and nucleus accumbens segmentations of that hemisphere.

In the growing phase of GAMEs a reference mesh for both left and right striatum was generated. First, a voxel-wise spatial probability map of the segmentation masks of the MC group was generated, by voxel counting at each voxel location. Voxels labeled as striatum in more than 20% of the MC masks formed the average segmentation volume, which formed the basis on which a mesh was grown. This threshold was chosen based on visual comparison of different meshes built with different thresholds (ranging from 10%–90%). We found thresholds above 60% to loose shape characteristics of the striatum, and thresholds below 15% needed exponentially more nodes to form the reference mesh. We assumed that a relatively large reference model would represent the "healthy" shape of the striatum, least affected by degenerative processes accompanying age. Therefore, a low threshold (20%) was chosen to create a relatively large reference model, but for

which approximately an average amount of nodes was needed to form the model (i.e., 605 for the left striatum and 645 for the right striatum). Accuracy for the mesh was set at 2 mm isotropic per node: considering that T1 structural images were normalized to 1 mm isotropic, higher resolutions would approach the voxel resolution, thus being meaningless. This reference mesh topology was frozen to keep the number of nodes and edges constant in the following steps.

In phase two of GAMEs, the reference mesh was adapted to all striatal segmentation masks of both 35 MCs and 35 AD patients, thus 70 meshes for each striatal hemisphere were generated. The adaptation was based on the topology-preserving Kohonen self-organizing map algorithm (1990). The outcome of GAMEs was a set of comparable meshes, also defined as a 3D Point Distribution Model (PDM). In this model each node (i.e., location) of the mesh had corresponding nodes through all other instances and therefore the meshes were locally comparable. Previous work has shown that corresponding nodes of meshes generated with GAMEs are indeed representative of similar anatomical locations (Ferrarini, Palm, et al. 2008).

Statistical analysis of local shape differences between MCs and AD-patients Local shape differences between the MCs and AD patients were assessed using non-parametric repeated permutation tests and a bootstrapping technique (Ferrarini, Palm, et al. 2008). The advantage of repeated tests on bootstrapped subsamples is to reduce the bias of the results to the particular subjects included in the analysis. This leads to statistically more robust results, since only those locations are identified that are systematically different for different subsamples of the MC and AD group. Bootstrapping was set to 60% of the study sample, i.e., the entire set of $35 + 35$ subjects was randomly subsampled to $21 + 21$ subjects, and this was repeated 25 times ($N^{iter} = 25$).

Permutation tests were performed for each subsampled set (with the number of permutations set at $10,000$). Each node in the 3D PDM was surrounded by two 3D clouds of 21 points (one cloud per study group). Non-parametric permutation tests were applied in case part of nodes was surrounded by clouds of points that were not normally distributed. Hotelling's T^2 statistic (HT^2) was used (1931), which is a simple generalization to multidimensional data of the Student's t-test. First, the average location and covariance matrix of each cloud were evaluated, from which the HT^2 statistic for the two groups was estimated (HT^2_{original}). Subsequently, the groups were randomly mixed $10,000$ times, and for each time the corresponding Hotelling's (HT^2) statistic was calculated (HT^2_i , $i = 1.10000$). The distribution of the HT^2_i respects the null hypothesis for the two clouds to come from the same distribution. The percentage of HT^2_i values higher than (HT^2_{original}) was considered the p-value for the given node. Repeating this procedure for each node resulted in a p-value map, in which each mesh node was given a

p-value for the null hypothesis that the two groups had similar local shape distributions in space. Given the entire set of 25 p-maps, the median p-value per node was evaluated. A p-value $\leqslant 0.05$ for a node was considered significant. Moreover, a consistency index (CI) per node was assessed, representing the frequency a given node was found significantly different over the 25 iterations. The direction and length of the displacement vectors, needed to deform the average shape of the striatum of the MC population into the average shape of striatum of the AD population, were also estimated.

To ascertain that surface deformity was due to the pathology investigated and not to shifting of the whole structure, the centers of gravity between the groups were compared. Differences in center of gravity were nonsignificant and within the width of one voxel.

Assessment of the relation of striatal surface deformity with cognitive performance For each node location, the principal component of the associated cloud of points, consisting of 35 points for AD and 35 for MCs, was estimated. Subsequently, each point of the cloud was projected along the main eigenvector, with positive projections (with respect to the reference node on the reference mesh) pointing inwardly. The projection lengths around the reference nodes were tested on normality with the Lilliefors test (Lilliefors 1967). For each striatal hemisphere, approximately 25% of the nodes were not normally distributed ($p < 0.05$), however locations of not normally distributed point clouds were dispersed over the surface (figure 1) and applying false discovery rate corrections proved all the p-values to be nonsignificant. We therefore proceeded with a linear regression analysis. First, the CAMCOG-R score was regressed against age, gender, educational level, and BPV in a linear model. The residuals from these models were then linearly regressed against the projection lengths around each striatal surface node. Note that the projection lengths were calculated in standard space and thus normalized for head size. The direction, positive or negative, of the association of surface deformity with cognitive score was determined, together with r^2 and p-values of the model. A $p \leqslant 0.05$ was considered significant.

RESULTS

Group characteristics

Successful matching of the study groups MCs and AD was verified; no significant differences in age, gender, educational level, and scaling factor for head size normalization were found (table 1). Groupwise differences existed in total CAMCOG-R score and all subscores ($t = 8.4$, $df = 39$, $p < 0.001$), BPV ($t = 2.2$, $df = 68$, $p = 0.03$), total volumes of left ($t = 2.0$, $df = 61$, $p = 0.048$) and right striatum ($t = 2.2$, $df = 68$,

Figure 1: Normality of the point distributions surrounding the striatal surface nodes

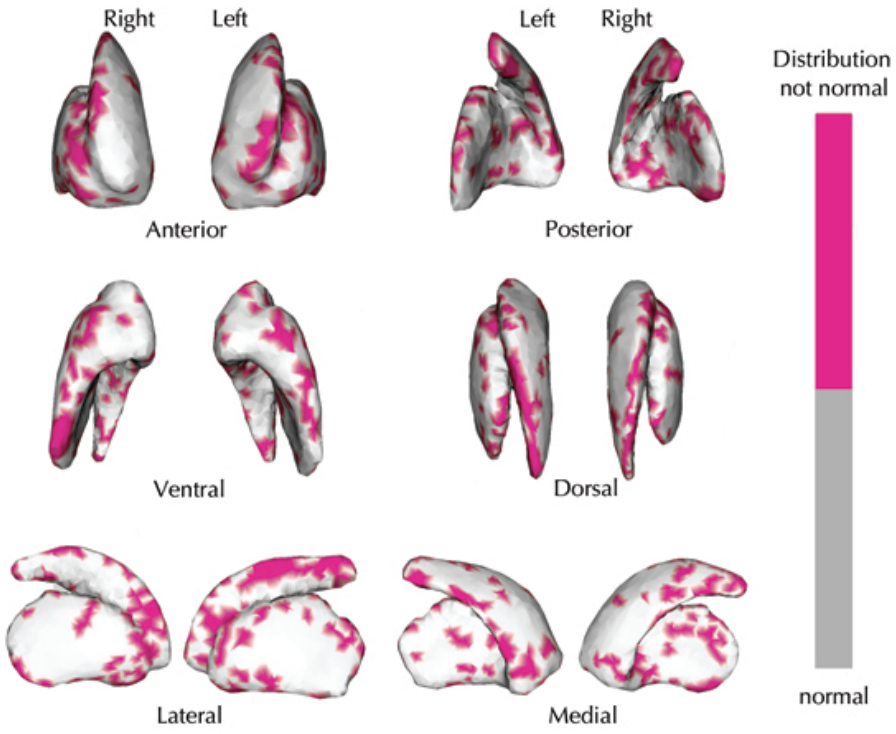

The distributions of the point clouds surrounding each node on the surface of the striatum that were not normally distributed are colored red. Normality was tested with the Lilliefors test. 25% of the point clouds of the left striatum were not normally distributed and 24% of the right striatum (p-value < 0.05). Applying false discovery rate corrections proved all p–values to be not significant.

$p = 0.03$), and volume of left putamen ($t = 2.9$, $df = 63$, $p = 0.004$). Mean volumes of left and right caudate, right putamen, and left and right accumbens were smaller in AD, but did not reach statistical difference.

Table 1: Demographics & group characteristics

	MCs ($n = 35$) Mean (SE)	AD ($n = 25$) Mean (SE)	Two-sample unpaired t-test t-value (df)	Cohen's d Effect size
Age in years	72.4 (1.4)	73.1 (1.4)	0.31 (68)	0.07
Sex (Male : Female)	15:20	15:20	0 (68)	0.00
Education	11.2 (0.6)	10.0 (0.7)	−1.20 (64)	−0.29
Scaling factor[a]	1.33 (0.02)	1.34 (0.02)	−0.21 (67)	−0.05
CAMCOG-R	89.1 (0.9)	62.7 (2.8)	−8.36 (38)***	−1.44
Subscores:				
Orientation	9.1 (0.1)	6.5 (0.4)	−5.55 (40)***	−1.11
Language	26.5 (0.3)	21.3 (0.7)	−5.92 (44)***	−1.17
Memory	21.1 (0.4)	12.3 (1.0)	−7.60 (43)***	−1.34
Attention	6.3 (0.1)	3.8 (0.4)	−5.59 (40)***	−1.13
Visuo	5.1 (0.1)	2.8 (0.3)	−7.15 (46)***	−1.33
Executive	14.5 (0.4)	8.0 (0.7)	−7.71 (53)***	−1.38
Brain parenchyma	1449 (16.1)	1397 (17.0)	−2.23 (68)*	−0.52
Striatum L	13.2 (0.2)	12.4 (0.3)	−2.01 (61)*	−0.47
Striatum R	14.3 (0.2)	13.5 (0.2)	−2.20 (68)*	−0.51
Caudate nucleus L	5.5 (0.2)	5.4 (0.2)	−0.34 (65)	−0.08
Caudate nucleus R	6.3 (0.2)	5.9 (0.2)	−1.66 (68)	−0.39
Putamen L	7.0 (0.1)	6.4 (0.2)	−2.94 (63)**	−0.67
Putamen R	7.5 (0.1)	7.2 (0.2)	−1.49 (65)	−0.35
N accumbens L	0.68 (0.04)	0.61 (0.03)	−1.44 (65)	−0.34
N accumbens R	0.49 (0.03)	0.43 (0.03)	−1.20 (68)	−0.29

MCs, memory complainers; AD, Alzheimer patients; CAMCOG-R: Cambridge cognition examination Revised; BPV, total brain parenchymal volume; Striatum, consists of caudate nucleus, putamen, and nucleus accumbens; L, Left; R, Right

a Scaling factor, used to normalize for head size

All volumes are in cm^3 and normalized for head size;

*** p-value < 0.0005; ** p-value < 0.005; * p-value < 0.05.

Local atrophy of the striatum in AD patients

Figure 2 summarizes the results of shape comparison between MCs and AD patients. Red colored areas were significantly different ($p < 0.05$) in $> 95\%$ of the repeated permutation tests, orange areas in $> 90\%$ of the tests, and yellow areas in $> 80\%$ of the tests. Symmetrical locations of significant consistent shape differences appeared in

Figure 2: Areas of significant striatal surface change in AD compared to MC

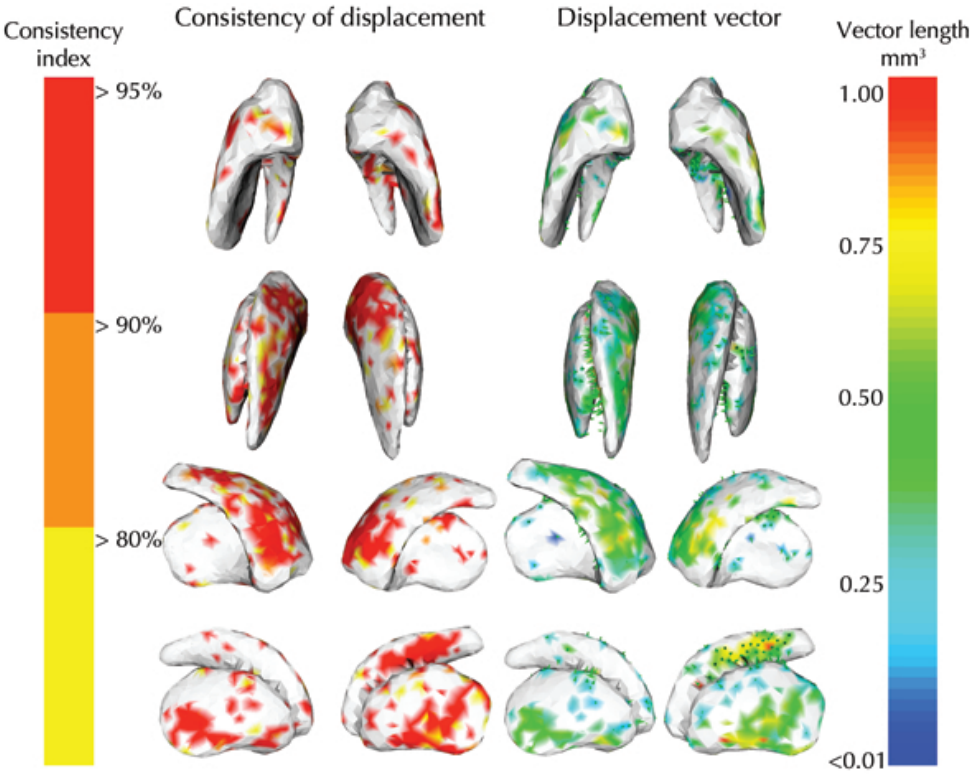

Consistency of displacement: the colored surface areas were significantly ($p < 0.05$) deformed in AD patients compared to MCs. Red areas were significantly different in more than 95% of the 25 iterations of the permutation tests, orange in more than 90%, and yellow in more than 80%.
Displacement vector: the length of the displacement vectors, needed to deform the surface of MC to AD, was color coded with red indicating a length of $\leqslant 1.00$ mm to dark blue indicating < 0.01 mm. Outwardly directed displacement vectors were represented by green arrows on the surface. The displacement vectors of the lateral putamen and medial caudate were directed inwards.

both striatal hemispheres, i.e., the rostral medial caudate nucleus and ventral lateral putamen. Shape deformity in the left striatal hemisphere, however was more extended, i.e., 30.4% of total surface compared to 21.1% of the right hemisphere. On the left

striatum, areas of shape deformity on the caudate nucleus covered the medial wall with the largest confluent area on the ventral half of the caudate head and a smaller area on the lateral side of the caudate body. The left putamen showed areas of shape difference on the lateral side of the putamen, with the largest confluent areas on the ventral half. On the right striatum confluent areas of difference were found on the medial caudate head and ventral half of the lateral putamen. In both hemispheres, the medial sides of the putamen and the accumbens areas were virtually devoid of significant shape difference between the groups. Outward directions of the vector displacement of the surface nodes were displayed in green arrows. All areas of shape deformity were inwardly directed, except a small area on the left lateral caudate nucleus with outwardly directed arrows. The length of the displacement vectors were color coded showing the largest shape deformity in the ventral parts of the lateral putamen and in the caudate head between MCs and AD.

Table 2: Correlation of striatal volumes with CAMCOG-R score

		All subjects (n=70)		MC (n=35)		AD (n=35)	
		R^a	R^b	R^a	R^b	R^a	R^b
Striatum	L	0.41***	0.28*	0.03	−0.18	0.40*	0.24
	R	0.25*	0.13	−0.12	−0.27	0.10	−0.04
Caudate nucleus	L	0.18	0.08	−0.02	−0.09	0.21	0.06
	R	0.10	0.02	−0.15	−0.17	−0.13	−0.23
Putamen	L	0.52***	0.41**	0.06	−0.18	0.51***	0.38*
	R	0.27*	0.19	−0.10	−0.29	0.24	0.16
Accumbens	L	0.18	0.09	0.06	−0.17	0.07	−0.02
	R	0.21	0.13	0.23	−0.01	0.20	0.11

CAMCOG-R score, Cambridge cognition examination revised; L, Left; R, Right

[a] Adjusted for age, gender, education in years, and head size.

[b] Adjusted for age, gender, education in years, head size, and BPV.

*** p-value < 0.0005; ** p-value < 0.005; * p-value < 0.05.

Relation of striatal volumes and cognition

In the total sample CAMCOG-R score significantly decreased with decreasing volumes of total left striatum ($r = 0.41$, $p < 0.001$, total right striatum ($r = 25$, $p = 0.04$), left putamen ($r = 0.52$, $p < 0.001$), and right putamen ($r = 0.27$, $p = 0.03$). These associations were adjusted for age, gender, years of education, and head size. After additional correction for BPV decreasing CAMCOG-R score remained significantly related

to decreasing volumes of total left striatum ($r = 0.28$, $p = 0.02$) and left putamen ($r = 0.41$, $p < 0.001$). Performing the analysis separately for each group, associations of cognitive score with volume of the total left striatum ($r = 0.40$, $p = 0.02$) and left putamen ($r = 0.51$, $p = 0.003$) were found in the AD group, but no significant associations in the MC group (see table 2).

Relation of striatal shape and cognitive

Similar locations of surface deformity that associated with cognitive performance existed in both striatal hemispheres, after corrections for age, gender, years of education, BPV, and head size. The areas were, however, more extended on the left side with 40.1% of the total surface relating significantly to cognitive performance compared to 29.1% of the right striatal surface (figure 3). CAMCOG-R score in this study population positively related to surface deformity on the medial ventral caudate, lateral putamen, and accumbens areas. Strongest correlations were found on the left side with r^2 ranging from 0.05 to 0.30 and on the right with r^2 ranging from 0.05 to 0.27. The dorsal areas of the caudate and putamen, and the medial putamen did not significantly relate to CAMCOG-R score.

DISCUSSION

In this combined volumetric and morphometric analysis, shape abnormalities were observed in AD patients in the rostral medial caudate head and the ventral and lateral putamen when compared to memory complainers with normal cognitive test scores. This suggests that AD pathology predominantly affects the limbic and associative areas of the striatum. Furthermore, cognitive impairment related to the degree of surface deformity in the ventral areas of the caudate and putamen, and the accumbens area, but not to the dorsal areas. This association may be based on degenerative process in cognitively functional parts of the striatum or based on the disruption of the networks in which the striatum takes part. Atrophy of the striatum in AD has been described before, however, here we report on the occurrence of shape abnormalities selectively occurring in the ventral parts of the striatum and its relation to cognition. Our results are in agreement with multiple studies showing manifestation of AD pathology preferentially in the limbic and associative areas of the cerebrum (H Braak and E Braak 1991; Savioz et al. 2009). The present study design, however, is not suitable to dissociate an independent effect of striatal atrophy on cognitive symptoms in AD. Future studies are needed to assess whether striatal deformation is an early or late phenomenon in the development

Figure 3: Locations of striatal shape deformity related to cognitive performance

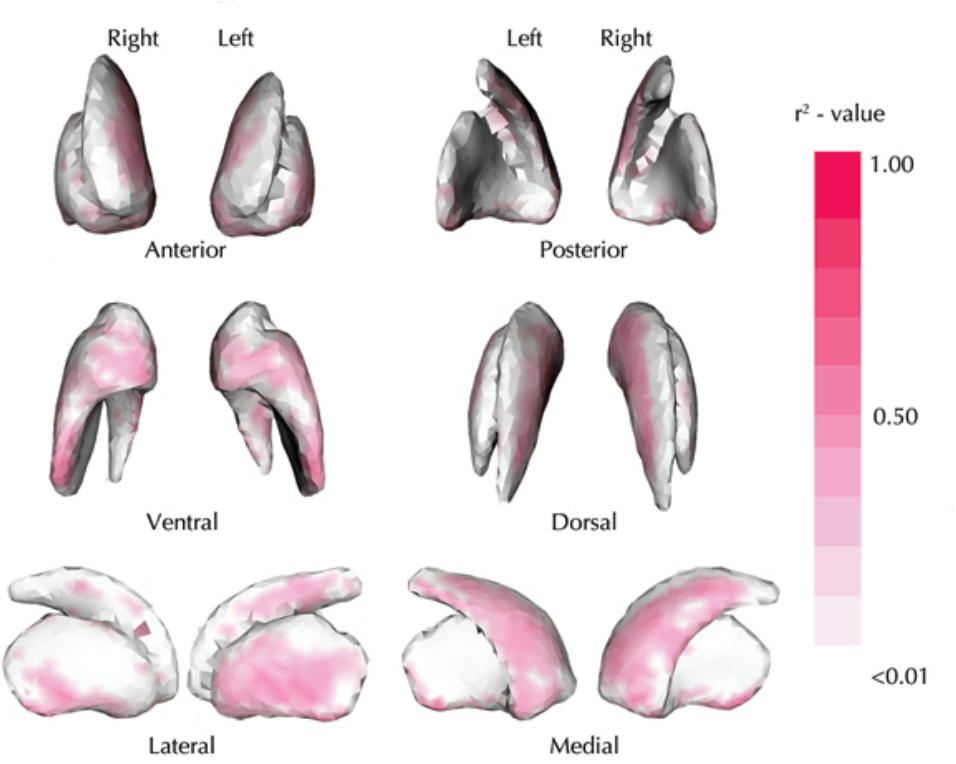

Surface areas of the striatum of which deformity significantly associated with CAMCOG-R score were colored red. All associations observed were negatively directed, meaning an increasing inward shape deformity in these areas related to a decreasing cognitive score. The *r*-value, estimated from a linear model corrected for age, gender, education in years, head size, and BPV for each surface node, was color coded with different shadings of red. Peak r^2 for the left striatum was 0.30 and for the right striatum 0.27. Forty percent of the left striatal surface associated significantly with CAMCOG-R score and 29% of the right striatum.

of AD and whether markers for striatal degeneration can improve risk prediction for AD in older people.

Selective degeneration of the striatum in AD is likely to underlie regional shape deformity found in the ventral caudate and putaminal areas. In histological studies on AD, a loss of the large cholinergic neurons was predominantly observed in the ventral stria-

tum. Neurofibrillary tangles were observed in the remaining cholinergic cells throughout the striatum (Oyanagi et al. 1987). The cholinergic interneuron network has extended arborizations and is tonically active (Wilson, Chang, and Kitai 1990). Moreover, it has been proposed that this network influences the activity of the entire striatum (Graybiel et al. 1994). The large cholinergic interneurons, however, are only a minority (1–2%) of all striatal cell types (Bolam, Wainer, and AD Smith 1984) and consequently, selective loss of these cells may not fully explain the significant surface deformity observed in this study. Another possible explanation for the observed shape deformity in the striatum in AD may be the presence of amyloid plaques triggering increased neural cell death in the striatum. Accumulation of amyloid in the striatum has been observed across different autosomal Alzheimer disease mutation types (Klunk et al. 2007; Villemagne et al. 2009) and related to loss of medium size spiny neurons in 12-month old APPswe/PS1ΔE9 transgenic mice compared to their wild type peers (Richner, Bach, and West 2009). Shape deformity could also be due to Wallerian degeneration following damage in other regions of the brain that are structurally connected to the striatum. Supportive for this hypothesis is a post mortem analysis of 20 cases observing that the occurrence of striatal changes paralleled the occurrence of neuritic plaques in the neocortex (Wolf et al. 1999).

Significant associations with cognitive decline were observed in the rostral medial caudate, ventral lateral putamen, but also in the nucleus accumbens. Previous studies have assigned reward and reinforcement learning tasks to the ventral striatum (Graybiel 2008; Haber and McFarland 1999) and together with the basolateral and extended amygdala the ventral striatum seems to be essential for stimulus associations to rewarding consequences of behavior (Gray 1999). Also, evidence is accumulating for anatomical substrates of incentive learning and habit formation in the rostral ventral parts of the caudate and putamen (Haber, Kim, et al. 2006). Atrophy of the putamen and the caudate nucleus has been related to the occurrence of neuropsychiatric symptoms in AD by others (Mega et al. 2000; Bruen et al. 2008). Our study shows that the areas of which deformity relates to cognitive impairment and AD are confined to the ventral parts of the putamen and caudate. Although, both volumetric and morphometric analysis were performed with corrections for global brain tissue volume, cognitive symptoms may still arise due to dysfunction elsewhere in the limbic and associative circuits in which the striatum takes part. The medial rostral part of the caudate nucleus and the rostral ventral putamen receive projections from the ventral medial prefrontal, orbitofrontal, and dorsal anterior cingulate cortices (Haber 2003), areas that are more affected in AD than other parts of the brain (Callen et al. 2001). Results of both volumetric and morphometric analyses show shape deformity and volume loss of the putamen in AD. The area of the ventral striatum caudal to the anterior commissure has not been studied extensively,

but a study on primates observed that this region is also part of the limbic striatum with afferents from the amygdala and a similar histochemical and cellular organization as the anterior ventral striatum (Fudge and Haber 2002). Also, part of the posterior ventral putamen, is regarded as the "visual striatum" forming a closed loop with the TE visual area of the inferotemporal lobe (Middleton and Strick 1996).

Another interesting finding of our study was the larger area of shape deformity and association with cognitive impairment in the left striatum, compared to the right. This is in agreement with several studies that described hemispherical asymmetrical findings for the hippocampus and orbitofrontal lobes in AD (Barnes et al. 2005; Raji et al. 2008). Also, our study included only right-handed persons, which may have increased the hemispherical dissimilarity.

We hypothesized that the entire limbic ventral striatum atrophies in AD, however, no difference of shape between AD and MC of the nucleus accumbens, which is part of the ventral striatum, was found. The nucleus accumbens is an essential part of the limbic striatum, receiving afferents from the ventral medial prefrontal cortex, amygdala, and hippocampus and integrating the information from these cortices (Gruber, Hussain, and O'Donnell 2009). We did find a relation of deformity of the accumbens with cognitive impairment. Shape deformity of the accumbens in AD cannot be excluded, based on these results only. There is evidence that part of the memory complainers have early stages of AD and may suffer striatal atrophy to a degree that diminishes the differences between the studied groups. Also, it may be that not all AD patients suffer shape abnormalities in the area of the accumbens or that our method is not sensitive enough for detection of shape deformity in this area.

Our results demonstrate the additional value of morphometric analysis as compared to a volumetric analysis in assessing changes in the striatum in AD patients. With volumetric analysis only, associations with cognitive decline were limited to the putamen. The morphological data also showed 1) shape deformity in the caudate nucleus, which associated with cognitive impairment and 2) localized shape deformity in especially the ventral half of the right putamen.

Lastly, some methodological limitations are of note. First, we used cross-sectional data for our determination of shape abnormalities in the striatum. Longitudinal data are needed to determine whether the shape deformity in the basal ganglia is a late or early phenomenon in the development AD and reflecting volume loss. Longitudinal data would also help assessing whether atrophy of the basal ganglia is primary or secondary to atrophy in other (limbic) brain regions, such as the hippocampus. The second important limitation of our study is that our control group consisted of memory complainers. Several studies revealed the presence of smaller left hippocampal volumes and decreased gray matter volumes among memory complainers, suggesting that this condition is an

early stage of AD in some patients (van der Flier et al. 2004; Saykin et al. 2006). However, the memory complainers form a relevant control group from a clinical perspective, since AD subjects need to be distinguished from MC and MCI cases. Also, if AD pathology is present, it is likely to be less pronounced than in demented patients, and the extent of striatal deformity may have been underestimated. A third limitation is that the CAMCOG-R score is a screening test for cognitive impairment and is not specifically aimed at detecting basal ganglia dysfunction. Future studies are needed to assess whether a specific cognitive function is affected by striatal atrophy in AD.

In conclusion, morphometric analysis of the striatum shows the occurrence of shape deformity in AD predominantly in the rostral medial part of the caudate nucleus and ventral lateral putamen in AD patients. These areas are known to participate in circuits with the medial temporal lobe and prefrontal cortex and were associated with cognitive impairment. Shape deformity of the accumbens was also associated with cognitive impairment, but was not significantly different between MCs and AD patients.

BIBLIOGRAPHY

Barnes J, Scahill RI, Schott JM, Frost C, Rossor MN, and Fox NC (2005). "Does Alzheimer's disease affect hippocampal asymmetry? Evidence from a cross-sectional and longitudinal volumetric MRI study". *Dement. Geriatr. Cogn. Disord.* 19 (5-6): 338–344. DOI: 10.1159/000084560.

Bhatia KP and Marsden CD (1994). "The behavioural and motor consequences of focal lesions of the basal ganglia in man". *Brain* 117 (4): 859–876. DOI: 10.1093/brain/117.4.859.

Bolam JP, Wainer BH, and Smith AD (1984). "Characterization of cholinergic neurons in the rat neostriatum. A combination of choline acetyltransferase immunocytochemistry, Golgi-impregnation and electron microscopy". *Neuroscience* 12 (3): 711–718. DOI: 10.1016/0306-4522(84)90165-9.

Braak H and Braak E (1991). "Alzheimer's disease affects limbic nuclei of the thalamus". *Acta Neuropathol.* 81 (3): 261–268. DOI: 10.1007/BF00305867.

Bruen PD, McGeown WJ, Shanks MF, and Venneri A (2008). "Neuroanatomical correlates of neuropsychiatric symptoms in Alzheimer's disease". *Brain* 131 (9): 2455–2463. DOI: 10.1093/brain/awn151.

Callen DJ, Black SE, Gao F, Caldwell CB, and Szalai JP (2001). "Beyond the hippocampus: MRI volumetry confirms widespread limbic atrophy in AD". *Neurology* 57 (9): 1669–1674. DOI: 10.1212/WNL.57.9.1669.

de Jong LW, van der Hiele K, Veer IM, Houwing JJ, Westendorp RG, et al. (2008). "Strongly reduced volumes of putamen and thalamus in Alzheimer's disease: an MRI study". *Brain* 131 (12): 3277–3285. DOI: 10.1093/brain/awn278.

Ferrarini L, Olofsen H, Palm WM, van Buchem MA, Reiber JH, and Admiraal-Behloul F (2007). "GAMEs: growing and adaptive meshes for fully automatic shape modeling and analysis". *Med. Image Anal.* 11 (3): 302–314. DOI: 10.1016/j.media.2007.03.006.

Ferrarini L, Palm WM, Olofsen H, van der Landen R, van Buchem MA, et al. (2008). "Ventricular shape biomarkers for Alzheimer's disease in clinical MR images". *Magn. Reson. Med.* 59 (2): 260–267. DOI: 10.1002/mrm.21471.

Fudge JL and Haber SN (2002). "Defining the caudal ventral striatum in primates: cellular and histochemical features". *J. Neurosci.* 22 (23): 10078–10082. URL: http://www.jneurosci.org/content/22/23/10078 (visited on 09/10/2018).

Gearing M, Levey AI, and Mirra SS (1997). "Diffuse plaques in the striatum in Alzheimer disease (AD): relationship to the striatal mosaic and selected neuropeptide markers". *J. Neuropathol. Exp. Neurol.* 56 (12): 1363–1370. DOI: 10.1097/00005072-199712000-00011.

Gerfen CR (1992). "The neostriatal mosaic: multiple levels of compartmental organization in the basal ganglia". *Annu. Rev. Neurosci.* 15: 285–320. DOI: 10.1146/annurev.ne.15.030192.001441.

Gray TS (1999). "Functional and anatomical relationships among the amygdala, basal forebrain, ventral striatum, and cortex. An integrative discussion". *Ann. N. Y. Acad. Sci.* 877: 439–444. DOI: 10.1111/j.1749-6632.1999.tb09281.x.

Graybiel AM (2008). "Habits, rituals, and the evaluative brain". *Annu. Rev. Neurosci.* 31: 359–387. DOI: 10.1146/annurev.neuro.29.051605.112851.

Graybiel AM, Aosaki T, Flaherty AW, and Kimura M (1994). "The basal ganglia and adaptive motor control". *Science* 265 (5180): 1826–1831. DOI: 10.1126/science.8091209.

Gruber AJ, Hussain RJ, and O'Donnell P (2009). "The nucleus accumbens: a switchboard for goal-directed behaviors". *PLoS ONE* 4 (4): e5062. DOI: 10.1371/journal.pone.0005062.

Haber SN (2003). "The primate basal ganglia: parallel and integrative networks". *J. Chem. Neuroanat.* 26 (4): 317–330. DOI: 10.1016/j.jchemneu.2003.10.003.

Haber SN, Kim KS, Mailly P, and Calzavara R (2006). "Reward-related cortical inputs define a large striatal region in primates that interface with associative cortical connections, providing a substrate for incentive-based learning". *J. Neurosci.* 26 (32): 8368–8376. DOI: 10.1523/JNEUROSCI.0271-06.2006.

Haber SN and McFarland NR (1999). "The concept of the ventral striatum in nonhuman primates". *Ann. N. Y. Acad. Sci.* 877: 33–48. DOI: 10.1111/j.1749-6632.1999.tb09259.x.

Hall AM, Moore RY, Lopez OL, Kuller L, and Becker JT (2008). "Basal forebrain atrophy is a presymptomatic marker for Alzheimer's disease". *Alzheimers. Dement.* 4 (4): 271–279. DOI: 10.1016/j.jalz.2008.04.005.

Herrero MT, Barcia C, and Navarro JM (2002). "Functional anatomy of thalamus and basal ganglia". *Childs Nerv. Syst.* 18 (8): 386–404. DOI: 10.1007/s00381-002-0604-1.

Hotelling H (1931). "The generalization of 'Student's' ratio." *Ann. Math. Statist.* 2 (3): 360–378. DOI: 10.1214/aoms/1177732979.

Karas GB, Burton EJ, Rombouts SA, van Schijndel RA, O'Brien JT, et al. (2003). "A comprehensive study of gray matter loss in patients with Alzheimer's disease using optimized voxel-based morphometry". *Neuroimage* 18 (4): 895–907. DOI: 10.1016/S1053-8119(03)00041-7.

Klunk WE, Price JC, Mathis CA, Tsopelas ND, Lopresti BJ, et al. (2007). "Amyloid deposition begins in the striatum of presenilin-1 mutation carriers from two unrelated pedigrees". *J. Neurosci.* 27 (23): 6174–6184. DOI: 10.1523/JNEUROSCI.0730-07.2007.

Kohonen T (1990). "The self-organizing map". *Proc. IEEE* 78 (9): 1464–1480. DOI: 10.1109/5.58325.

Landau SM, Lal R, O'Neil JP, Baker S, and Jagust WJ (2009). "Striatal dopamine and working memory". *Cereb. Cortex* 19 (2): 445–454. DOI: 10.1093/cercor/bhn095.

Lilliefors HW (1967). "On the Kolmogorov-Smirnov test for normality with mean and variance unknown". *J. Am. Stat. Assoc.* 62 (318): 399–402. DOI: 10.2307/2283970.

McKhann G, Drachman D, Folstein M, Katzman R, Price D, and Stadlan EM (1984). "Clinical diagnosis of Alzheimer's disease: report of the NINCDS-ADRDA Work Group under the auspices of Department of Health and Human Services Task Force on Alzheimer's Disease". *Neurology* 34 (7): 939–944. DOI: 10.1212/WNL.34.7.939.

Mega MS, Lee L, Dinov ID, Mishkin F, Toga AW, and Cummings JL (2000). "Cerebral correlates of psychotic symptoms in Alzheimer's disease". *J. Neurol. Neurosurg. Psychiatr.* 69 (2): 167–171. DOI: 10.1136/jnnp.69.2.167.

Middleton FA and Strick PL (1996). "The temporal lobe is a target of output from the basal ganglia". *Proc. Natl. Acad. Sci. U.S.A.* 93 (16): 8683–8687. URL: http://www.pnas.org/content/pnas/93/16/8683.full.pdf (visited on 09/10/2018).

Oyanagi K, Takahashi H, Wakabayashi K, and Ikuta F (1987). "Selective involvement of large neurons in the neostriatum of Alzheimer's disease and senile dementia: a morphometric investigation". *Brain Res.* 411 (2): 205–211. DOI: 10.1016/0006-8993(87)91071-7.

Oyanagi K, Takahashi H, Wakabayashi K, and Ikuta F (1991). "Large neurons in the neostriatum in Alzheimer's disease and progressive supranuclear palsy: a topographic, histologic and ultrastructural investigation". *Brain Res.* 544 (2): 221–226. DOI: 10.1016/0006-8993(91)90057-3.

Parkinson J, Fudge J, Hurd Y, Pennartz C, and Peoples L (2000). "Finding motivation at Seabrook Island: the ventral striatum, learning and plasticity". *Trends Neurosci.* 23 (9): 383–384. DOI: 10.1016/S0166-2236(00)01644-1.

Patenaude B, Smith SM, Kennedy DN, and Jenkinson M (2007). *Bayesian shape and appearance models, FMRIB technical report TR07BP1*. London. URL: https://www.fmrib.ox.ac.uk/datasets/techrep/tr07bp1/tr07bp1.pdf (visited on 09/10/2018).

Poldrack RA and Packard MG (2003). "Competition among multiple memory systems: converging evidence from animal and human brain studies". *Neuropsychologia* 41 (3): 245–251. DOI: 10.1016/S0028-3932(02)00157-4.

R Core Team (2009). *R: A Language and Environment for Statistical Computing*. R Foundation for Statistical Computing. Vienna, Austria. URL: http://www.R-project.org/.

Raji CA, Becker JT, Tsopelas ND, Price JC, Mathis CA, et al. (2008). "Characterizing regional correlation, laterality and symmetry of amyloid deposition in mild cognitive impairment and Alzheimer's disease with Pittsburgh Compound B". *J. Neurosci. Methods* 172 (2): 277–282. DOI: 10.1016/j.jneumeth.2008.05.005.

Richner M, Bach G, and West MJ (2009). "Over expression of amyloid β-protein reduces the number of neurons in the striatum of APPswe/PS1ΔE9". *Brain Res.* 1266: 87–92. DOI: 10.1016/j.brainres.2009.02.025.

Roth M, Huppert FA, Mountjoy CQ, and Tym E (1988). *CAMDEX-R the Cambridge examination for mental disorders of the elderly*. Cambridge, UK: Cambridge University Press.

Savioz A, Leuba G, Vallet PG, and Walzer C (2009). "Contribution of neural networks to Alzheimer disease's progression". *Brain Res. Bull.* 80 (4-5): 309–314. DOI: 10.1016/j.brainresbull.2009.06.006.

Saykin AJ, Wishart HA, Rabin LA, Santulli RB, Flashman LA, et al. (2006). "Older adults with cognitive complaints show brain atrophy similar to that of amnestic MCI". *Neurology* 67 (5): 834–842. DOI: 10.1212/01.wnl.0000234032.77541.a2.

Smith SM, De Stefano N, Jenkinson M, and Matthews PM (2001). "Normalized accurate measurement of longitudinal brain change". *J. Comput. Assist. Tomogr.* 25 (3): 466–475. URL: http://journals.lww.com/jcat/Fulltext/2001/05000/Normalized_Accurate_Measurement_of_Longitudinal.22.aspx (visited on 09/10/2018).

Smith SM, Jenkinson M, Woolrich MW, Beckmann CF, Behrens TE, et al. (2004). "Advances in functional and structural MR image analysis and implementation as FSL". *Neuroimage* 23 Suppl 1: S208–219. DOI: 10.1016/j.neuroimage.2004.07.051.

Smith SM, Zhang Y, Jenkinson M, Chen J, Matthews PM, et al. (2002). "Accurate, robust, and automated longitudinal and cross-sectional brain change analysis". *Neuroimage* 17 (1): 479–489. DOI: 10.1006/nimg.2002.1040.

Utter AA and Basso MA (2008). "The basal ganglia: an overview of circuits and function". *Neurosci. Biobehav. Rev.* 32 (3): 333–342. DOI: 10.1016/j.neubiorev.2006.11.003.

van der Flier WM, van Buchem MA, Weverling-Rijnsburger AW, Mutsaers ER, Bollen EL, et al. (2004). "Memory complaints in patients with normal cognition are associated with smaller hippocampal volumes". *J. Neurol.* 251 (6): 671–675. DOI: 10.1007/s00415-004-0390-7.

Villemagne VL, Ataka S, Mizuno T, Brooks WS, Wada Y, et al. (2009). "High striatal amyloid β-peptide deposition across different autosomal Alzheimer disease mutation types". *Arch. Neurol.* 66 (12): 1537–1544. DOI: 10.1001/archneurol.2009.285.

Voorn P, Vanderschuren LJ, Groenewegen HJ, Robbins TW, and Pennartz CM (2004). "Putting a spin on the dorsal-ventral divide of the striatum". *Trends Neurosci.* 27 (8): 468–474. DOI: 10.1016/j.tins.2004.06.006.

Wilson CJ, Chang HT, and Kitai ST (1990). "Firing patterns and synaptic potentials of identified giant aspiny interneurons in the rat neostriatum". *J. Neurosci.* 10 (2): 508–519. URL: http://www.jneurosci.org/content/10/2/508 (visited on 09/10/2018).

Wolf DS, Gearing M, Snowdon DA, Mori H, Markesbery WR, and Mirra SS (1999). "Progression of regional neuropathology in Alzheimer disease and normal elderly: findings from the Nun study". *Alzheimer Dis. Assoc. Disord.* 13 (4): 226–231. URL: http://journals.lww.com/alzheimerjournal/Fulltext/1999/10000/Progression_of_Regional_Neuropathology_in.9.aspx (visited on 09/10/2018).

Yesavage JA and Sheikh JI (1986). "Geriatric depression scale (GDS) recent evidence and development of a shorter version". *Clin. Gerontol.* 5 (1-2): 165–173. DOI: 10.1300/J018v05n01_09.